# Effect of confinement on the liquid–liquid phase transition of supercooled water

**ARTICLE** *in* THE JOURNAL OF CHEMICAL PHYSICS · JULY 2007

Impact Factor: 2.95 · DOI: 10.1063/1.2734963 · Source: PubMed



**2 AUTHORS:**

Ivan V. Brovchenko
Technische Universität Dortmund
**92** PUBLICATIONS **1,648** CITATIONS
SEE PROFILE

Alla Oleinikova
Technische Universität Dortmund
**91** PUBLICATIONS **2,667** CITATIONS
SEE PROFILE

# Effect of confinement on the liquid-liquid phase transition of supercooled water

I. Brovchenko[a] and A. Oleinikova
*Physical Chemistry, University of Dortmund, Otto-Hahn-Str. 6, Dortmund D-44227, Germany*

(Received 27 November 2006; accepted 4 April 2007; published online 1 June 2007)

We report on an observation of the phase transition between two liquid phases of supercooled confined water in simulations. The temperature of the liquid-liquid transition of water at zero pressure slightly decreases due to confinement in the hydrophobic pore. The hydrophilic confinement affects this temperature in the opposite direction and shifts the critical point of the liquid-liquid transition to a higher pressure. As a result, in a strongly hydrophilic pore the liquid-liquid phase transition becomes continuous at zero pressure, indicating the shift of its critical point from negative to a positive pressure. These findings indicate that experimental studies of water confined in the pores of various hydrophobicity/hydrophilicity may clarify the location of the liquid-liquid critical point of bulk water. © *2007 American Institute of Physics*.
[DOI: 10.1063/1.2734963]

## I. INTRODUCTION

Apparent singular behavior of various properties of liquid water near 228 K (Ref. 1) may originate from the thermodynamic liquid-liquid phase transition between two water phases of different densities.[2] This hypothesis is supported by the experimental studies of the transitions between amorphous ices[3,4] and by the simulation studies of various water models.[2,5–8] Crystallization prevents direct experimental observation of this transition and, therefore, location of the hypothesized liquid-liquid critical point of water remains unknown. In simulations, location of the liquid-liquid phase transitions strongly depends on the water model and its implementation.[6] For example, the lowest-density liquid-liquid phase transition of a ST2 water model with the long-range Coulombic interactions in the form of a reaction field (ST2RF model hereafter)[2,6–8] ends in a critical point at a positive pressure. In this case, the anomalous behavior of liquid water upon cooling at zero pressure may be attributed to crossing the Widom line, which is defined as the locus of correlation length maxima emanating from the liquid-liquid critical point[7,8] (see dashed line and triangle in the left panel of Fig. 1). The critical point of the lowest-density liquid-liquid phase transition of the original ST2 water model[9] is located at negative pressure and liquid water undergoes a first-order phase transition upon cooling at zero pressure[5,6,10–12] (see asterisk in the left panel of Fig. 1). The critical pressure of the liquid-liquid phase transition in hydrogen bonded fluids shifts to higher pressures with the strengthening of the hydrogen bonds.[13] This indicates that the critical end point, where a critical liquid coexists with a noncritical vapor (see square in the left panel of Fig. 1), may be obtained by tuning the hydrogen bonding interactions in model water.

Crystallization of liquid water can be suppressed by confinement and the liquid-liquid transition of confined water was directly detected by experimental methods. In the incompletely filled pores, water undergoes a first-order phase transition at about 231–237 K in silica mesopores[14,15] and at about 240 K in Vycor glass.[16,17] Studies of water dynamics indicate, that this is a transition between two *liquid* water phases, which show quite different dynamical properties.[16,17] In cylindrical silica mesopores, water dynamics change drastically at about 225 K at zero pressure.[18–23] In more hydrophobic pores (carbon nanotubes), such dynamic transition of water occurs at a slightly lower temperatures (about 218 K[24]). At the surface of biomolecules, hydration water undergoes dynamic transition approximately at the same temperatures (222 and 220 K in the case of DNA[25] and lysozyme[26] molecules, respectively). Dynamic transition of water is closely related to the dynamic transition of biomolecules, which occurs in a rather narrow temperature interval (about 200–230 K) and is accompanied by the onset of biological function upon heating.[27,28]

It is natural to relate drastic changes of liquid water dynamics with the phase transition between two liquid phases with different properties. Moreover, we may expect qualitative changes of dynamics due to the continuous transition from one liquid to another in the supercritical region, as the critical point may affect the system properties in a wide thermodynamic range. The relation between the dynamic transition and liquid-liquid transition of confined water was proved directly in experiments with water in the incompletely filled pores.[16,17] In addition, similar to the liquid-liquid transition of water, the dynamic transition of confined water shifts to lower temperatures with increasing pressure.[19,20] Finally, recent simulations show close relation between the liquid-liquid transition of water and its dynamic transition.[8,29] Analysis of water dynamics above and below the transition temperature[8,18–22,29] leads to the idea, that upon cooling water undergoes a transition from a fragile liquid to a strong liquid.[30] This interpretation was questioned recently

[a]Electronic mail: brov@heineken.chemie.uni-dortmund.de

 

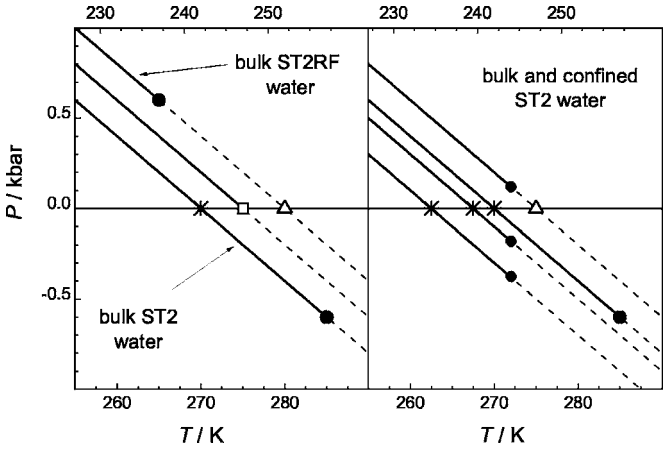


FIG. 1. Approximate location of the liquid-liquid critical points of bulk and confined water with respect to the liquid-vapor transition, shown by the horizontal line at $P=0$. Liquid-liquid phase transitions and corresponding Widom lines are shown by solid and dashed lines, respectively. Liquid-liquid critical points, liquid-liquid-vapor triple points and crossings of the Widom lines with the liquid-vapor transition are shown by circles, asterisks, and triangles, respectively. Left panel: ST2 water (Ref. 6). ST2RF water (Ref. 6) and the hypothetical model water, showing critical end point (square). Right panel: ST2 water in the pore with $U_0=-3.08$ kcal/mol, bulk water, water in the pore with $U_0=-1.93$ kcal/mol and $U_0=-0.39$ kcal/mol (from top to bottom). Liquid-liquid transitions of confined water are shown schematically, assuming bulk value $dP/dT$ and the same critical temperature in all pores. The upper temperature scale accounts for the temperature mismatch (−28°) (Ref. 6) between real and ST2 water.

(see Refs. 31–33 for more details). Obviously, a valuable conclusion concerning the origin of the specific temperature changes of water dynamics (both in experiments and in simulations) should be based on the knowledge of the phase diagram of water. The obtaining of such a phase diagram experimentally is problematic, and, therefore, simulation studies of the *phase diagram* of confined supercooled water may clarify the relation between the liquid-liquid and dynamic transition of liquid water. Clearly, these studies should precede any analysis of water dynamics.

The experimentally observed robustness of the liquid-liquid transition of water with respect to various confinements seems to be surprising, because usually the phase transitions of fluids are strongly effected by confinement. The density functional theory studies of the associating fluid show a strong effect of confinement on the liquid-liquid transition, which can be reduced only when the fluid is treated as homogeneous.[34] In the simulation studies of model water, the liquid-liquid transition of confined water was not found yet.[35,36] To understand the effect of confinement on the liquid-liquid phase transition of water, we have performed simulation studies of the liquid-vapor and first (lowest-density) liquid-liquid transition of model ST2 water in pores with various strengths of the water-wall interaction. Similarly to the previous studies of the liquid-liquid transition of water in confinement,[34–36] we used slitlike and not cylindrical pore geometry, which is more relevant to the cylindrical silica pores[18–23] and cylindrical carbon nanotubes,[24] used in experiments. This was done in order to avoid complications, caused by the smearing out of the phase transitions due to the one-dimensionality of cylindrical pores (effect of the pore geometry on the liquid-liquid transition of water deserves separate simulation studies). Besides, in the case of the incompletely filled Vycor glass[16,17] and hydrated biomolecules,[25,26] transition occurs in a water film, which is quasi-two-dimensional and in this respect is similar to a slit.

## II. SIMULATION METHODS

We studied phase diagram of ST2[9] water confined in slitlike pores with a width $H=24$ Å and periodic boundary conditions applied in two directions. Each structureless wall interacts with water oxygens via the long-range (9–3) Lennard-Jones potential, whose well-depth $U_0$ was varied to reproduce hydrophobic ($U_0=-0.39$ kcal/mol, paraffinlike surface), moderately hydrophilic ($U_0=-1.93$ kcal/mol, carbonlike surface), and strongly hydrophilic ($U_0=-3.08$ kcal/mol, silicalike surface) pores. A simple spherical cutoff $R_c=9$ Å of the intermolecular interactions was used. Contrary to the bulk case,[5,6] we did not use long-range corrections for Lennard-Jones intermolecular interactions in pore geometry. The effect of these corrections on the bulk phase diagram of ST2 water was found to be negligible at $T\geq 250$ K, whereas it causes increase of liquid water density on approximately 1.5% at lower temperatures.

Coexistence curves of the phase transitions of the confined ST2 water were obtained by Monte Carlo (MC) simulations in the Gibbs ensemble (GEMC).[37] In all pores we have simulated the liquid-vapor coexistence curve. Besides, the coexistence curve of the prewetting transition in the strongly hydrophilic pore and coexistence of two liquid water phases in hydrophobic and moderately hydrophilic pores were also studied by GEMC simulations. The use of efficient techniques for the molecular transfers[38] allows simulations of the liquid-vapor and liquid-liquid coexistence at $T\geq 200$ and $\geq 250$ K, respectively. The total number $N$ of molecules in the two simulation cells was about 850–1100 in the simulations of the liquid-vapor coexistence, about 500 in the simulations of the prewetting transition and about 1600 in the simulations of the liquid-liquid coexistence. The number of successful molecular transfers in the course of the simulation was about $10N-100N$ for liquid-vapor coexistence and prewetting transition and about $2N$ for liquid-liquid coexistence. The critical temperatures $T_c$ of the liquid-vapor and prewetting phase transitions of confined water were roughly estimated by the fitting the order parameter $\Delta\rho(T)$ of the transition (the difference between the densities of the coexisting phases) to the scaling law $\Delta\rho\sim\tau^{\beta}$, where $\tau=(T_c-T)/T_c$ is a reduced temperature deviation from the critical temperature and $\beta$ is an exponent. Note, that asymptotically close to the critical temperature of a fluid confined in a slitlike pore, the critical behavior is essentially two-dimensional and $\beta=0.125$. However, when the scaling law is applied to the temperature dependence of the order parameter in a wide range ($300\ \text{K}<T<T_c$ in our case), the exponent $\beta$ is just an effective fitting parameter, which may vary between the values of the critical exponent for two-dimensional (0.125) and three-dimensional (~0.326) systems. Critical density was estimated by fitting the coexistence curve diameter, that is the average density of two coexisting phases, by second-order polynomial.

To detect a possible liquid-liquid-vapor triple point, the liquid-vapor coexistence in the low-temperature region was calculated with a temperature step of 5 degrees. Due to hysteresis effects in the vicinity of the triple point, we simulated liquid-vapor coexistence by subsequent decrease of temperature, starting from some preequilibrated high-temperature configuration (typically at 300 K) and by subsequent increase of temperature, starting from some pre-equilibrated low-temperature configuration (typically 225–250 K). The temperature of the glassy transition of liquid water was estimated from the analysis of the temperature dependence of the potential energy along the liquid-vapor coexistence curve.

Structural properties of liquid water were studied by MC simulations of water in constant-volume ensemble at the densities, obtained from GEMC simulations. The density profiles of confined water were used to characterize distribution of water molecules in pores and to estimate a width of the first (surface) water layer. The structural properties of water were analyzed separately for the surface layer and for water in the pore center. The following properties were studied: Average density; oxygen-oxygen pair correlation function $g_{O-O}(r)$; and the fraction of water molecules with *NN* neighbors in the first coordination shell (number of molecules, whose oxygen atoms are situated closer then 3.5 Å to the oxygen atom of the considered water molecule). Besides, tetrahedral ordering of the nearest environment of a molecule was characterized by the tetrahedricity parameter $\theta$ (Ref. 39)

$$\theta = \sum_{i=1}^{5} \sum_{j=i+1}^{6} (l_i - l_j)^2 / (15\langle l \rangle^2), \tag{1}$$

where $l_i$ is the length of the $i$th edge of the tetrahedron with the oxygen atom of the studied molecule situated in its center and oxygen atoms of the four nearest water molecules situated in its vertices, $\langle l \rangle$ is the mean value of all its six edge lengths. This parameter measures a deviation of such constructed tetrahedron from the ideal one, which has $\theta = 0$.

## III. RESULTS

### A. Phase diagram of water in pores

The liquid-vapor coexistence curve of the ST2 water in the hydrophobic pore with $U_0 = -0.39$ kcal/mol is shown in Fig. 2. The critical temperature of the liquid-vapor transition of bulk ST2 water [approximately 550 K (Ref. 6)] shifts to about 530 K due to confinement in the hydrophobic pore. The liquid density along the liquid-vapor coexistence is shifted to lower values with respect to the bulk liquid due to the depletion of the liquid density near weakly attractive surfaces (see Refs. 40–42 for more details). Accordingly, the critical density also decreases from 0.286 g/cm$^3$ in the bulk to 0.214 g/cm$^3$ in the pore. The temperature of the liquid density maximum of bulk ST2 water is about 305 K.[6] In the hydrophobic pore, it shifts to an essentially lower temperature of about 275 K (Fig. 2).

The first (lowest-density) liquid-liquid phase transition of bulk ST2 water occurs in the equilibrium with a vapor phase (at almost zero pressure) at $T_t \approx 270$ K (Refs. 5 and 6)

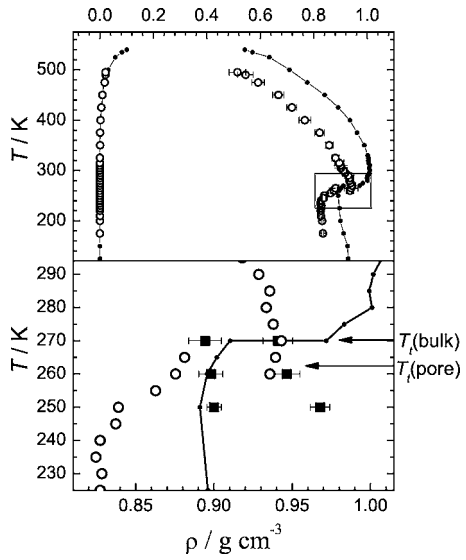


FIG. 2. Phase diagram of water in the pore with $U_0 = -0.39$ kcal/mol: Liquid-vapor coexistence (open circles), liquid-liquid coexistence (squares). The liquid-vapor coexistence curve of the bulk water is shown by solid circles and solid lines. The region boxed in the upper panel is shown in an enlarged scale in the lower panel.

(see horizontal step in the liquid branch of the coexistence curve of a bulk ST2 water in the lower panel of Fig. 2). The temperature of this liquid-liquid-vapor triple point decreases in the hydrophobic pore. At $T = 260$ K and $T = 265$ K, we have obtained coexistence between vapor and two liquid water phases of different densities, that clearly indicates liquid-liquid phase transition and its first-order character. This finding was confirmed by the direct equilibration of two coexisting liquid phases in the Gibbs ensemble at $T \geq 250$ K (see squares in the lower panel of Fig. 2). GEMC simulations does not give the value of the coexistence pressure.[37] The densities of two coexisting liquid phases shift to lower values with the increasing temperature, indicating that, similarly to the bulk case,[5,6] the slope $dP/dT$ of the liquid-liquid transition is negative. Due to the occurrence of a liquid-liquid-vapor triple point, this transition should end at the critical point at a negative pressure. The temperature $T_t$ of the liquid-liquid-vapor triple point may be estimated as the middle of the hysteresis loop, i.e., $T_t = 262.5 \pm 5$ K. Therefore, confinement in the hydrophobic pore shifts the temperature of the liquid-liquid-vapor triple point of the ST2 water to lower temperatures by just a few degrees. Similarly to the bulk case, at this temperature the liquid density in the pore shows a steplike decrease by about 0.05–0.06 g cm$^{-3}$.

The glass transition temperature $T_g$ of ST2 water in the pore was estimated from the temperature dependence of the potential energy $U$ per one water molecule (open circles in Fig. 3). Character of this dependence indicates, that transition at $T_t$ is a transition between two *liquid* phases, as it occurs above $T_g$, where the sharp drop of the heat capacity $\sim \partial U / \partial T$ occurs upon cooling. The temperature of the glass transition of water is not affected noticeably by the confinement in a hydrophobic pore (see Fig. 3).

The liquid-vapor coexistence curve of the ST2 water in the moderately hydrophilic pore with $U_0 = -1.93$ kcal/mol (Fig. 4) is qualitatively similar to that in hydrophobic pore

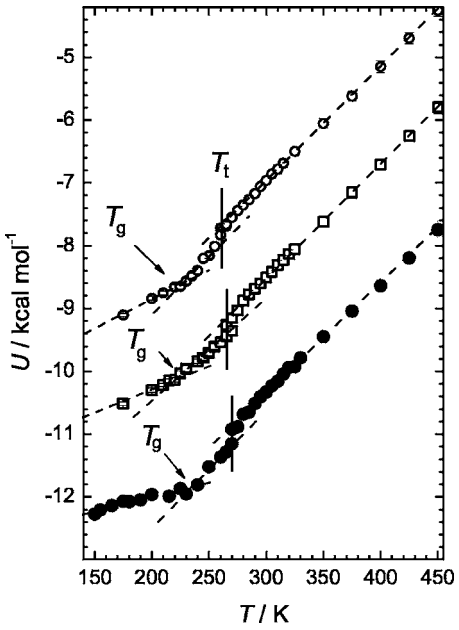


FIG. 3. Potential energy $U$ of a water molecule in the liquid phase along the liquid-vapor coexistence curve of bulk ST2 water (closed circles), ST2 water in the pores with $U_0=-1.93$ kcal/mol (open squares, shifted up by 2 kcal/mol) and $U_0=-0.39$ kcal/mol (open circles, shifted up by 3 kcal/mol). Vertical lines indicate liquid-liquid phase transition.

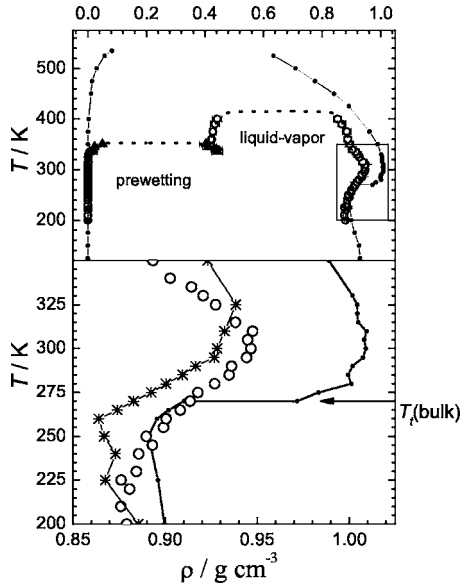


FIG. 5. Phase diagram of water in the pore with $U_0=-3.08$ kcal/mol: Liquid-vapor coexistence of water in the pore interior (open circles), prewetting transition (solid triangles). Dotted lines show the shape of the coexistence curve expected for 2D transitions. The liquid-vapor coexistence curve of the bulk water is shown by solid circles and solid lines. The region boxed in the upper panel is shown in an enlarged scale in the lower panel.

(Fig. 2). In accordance with theoretical expectations[43] and in agreement with previous simulation studies,[38,42] shift $\Delta T_c$ of the liquid-vapor critical temperature due to confinement is larger for the stronger water-wall interaction in the pore of the same size. Indeed, $\Delta T_c \sim 35$ K in the moderately hydrophilic pore, whereas $\Delta T_c \sim 20$ K in the hydrophobic pore. The critical density $\rho_c \sim 0.290$ g/cm$^{-3}$ of the liquid-vapor coexistence curve of water in the moderately hydrophilic pore practically coincides with the bulk value of $\rho_c \sim 0.286$ g/cm$^3$.[6]

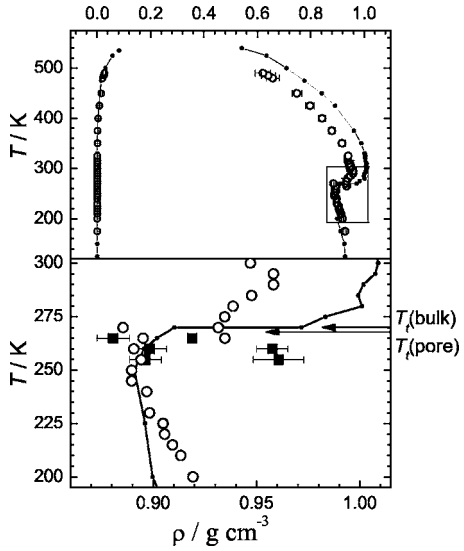


FIG. 4. Phase diagram of water in the pore with $U_0=-1.93$ kcal/mol: Liquid-vapor coexistence (open circles), liquid-liquid coexistence (squares). The liquid-vapor coexistence curve of the bulk water is shown by solid circles and solid lines. The region boxed in the upper panel is shown in an enlarged scale in the lower panel.

The temperature of the liquid density maximum of ST2 water shifts from 305 K to about 295 K due to confinement in the moderately hydrophilic pore, that is noticeably smaller, than due to confinement in the hydrophobic pore. We see coexistence of two liquid phases with a vapor at $T=265$ K and $T=270$ K (see lower panel in Fig. 4). This evidences first-order liquid-liquid phase transition with a liquid-liquid-vapor triple point at $T_t=267.5\pm5$ K, that is just slightly below the bulk value. This finding was confirmed by the direct equilibration of two coexisting liquid phases in the Gibbs ensemble at $T \geq 255$ K (see squares in lower panel of Fig. 4). The temperature dependence of $U$ in the moderately hydrophilic pore (see squares in Fig. 3) indicates that the glass transition temperature $T_g$ is noticeably below $T_t$. Thus, the phase transition at $T_t$ is a transition between two liquid phases. Despite the low accuracy in the estimation of $T_g$, we may notice shift of $T_g$ to lower temperatures due to confinement in this pore with respect to the bulk value $T_g \sim 235$ K [6] (see open squares in Fig. 3).

Strong water-wall interaction in the pore with $U_0=-3.08$ kcal/mol causes appearance of a prewetting transition, that a quasi-two-dimensional condensation of a finite water film at the pore surface (Fig. 5, solid triangles in the upper panel). Thickness of this water film is about two water layers, that is typical for water confined in hydrophilic nanopores.[38] At low temperatures, capillary condensation in such pores occurs in one step similarly to the condensation in more hydrophobic pores (Figs. 2 and 4). Starting from the temperature at about 340 K, water condensation occurs in two steps. First, the condensation of two water layers occurs via a prewetting transition. Second, capillary condensation occurs in the narrow pore with walls, covered by two water layers. The critical temperatures of these transitions are about 355 and 410 K, respectively. Above ~355 K, the

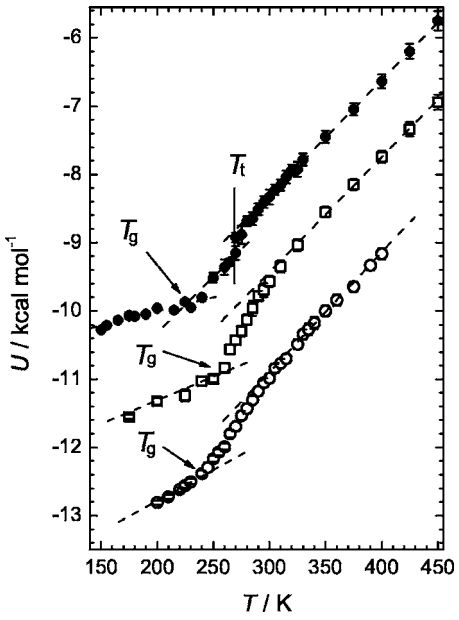


FIG. 6. Potential energy $U$ of a water molecule in the liquid phase along the liquid-vapor coexistence curve of ST2 water in the pores with $U_0=-3.08$ kcal/mol (open circles), bulk ST2 water (closed circles, shifted up by 2 kcal/mol), bulk ST2RF water (open squares, shifted up by 0.5 kcal/mol). The vertical line indicates liquid-liquid phase transition.

prewetting layer forms continuously. Note, that three water phases (vapor, two adsorbed water layers, and liquid) coexist at a temperature of ~340 K. In the case of a semi-infinite surface, this temperature corresponds to the temperature of a wetting transition.

The density of the liquid phase of ST2 water in a strongly hydrophilic pore with $U_0=-3.08$ kcal/mol changes gradually with temperature along the liquid-vapor coexistence and the liquid-liquid-vapor triple point is absent (Fig. 5, lower panel). This indicates the shift of the liquid-liquid critical point in hydrophilic pore from negative pressure to higher (positive) pressure. Such a pressure shift of the liquid-liquid critical point of the simple van der Waals model of hydrogen-bonded liquid may be achieved by strengthening the hydrogen bonds.[13] A similar shift of the liquid-liquid critical point was observed for the ST2RF water model, where the orientational ordering of water molecules was enhanced by the application of the long-range corrections for the Coulombic interaction[6] (see asterisks in the lower panel of Fig. 5). The Widom line, emanating from the liquid-liquid critical point located at a positive pressure, affects properties of liquid water at the liquid-vapor coexistence (see Fig. 1). The temperature, where the Widom line crosses the liquid-vapor phase transition, should be close to the heat capacity maximum of liquid water.[8] The temperature dependence of the potential energy of liquid water in a strongly hydrophilic pore is shown by open circles in Fig. 6. The maximum heat capacity corresponds to the maximum slope of this dependence and it is located at about 275 K, that is just slightly above the temperature of the liquid-liquid-vapor triple point of the bulk ST2 water. In the case of ST2RF water, this crossing temperature is about 280 K.[6,7] Although the liquid density maximum of ST2 water becomes much more pronounced in the strongly hydrophilic pore in comparison with

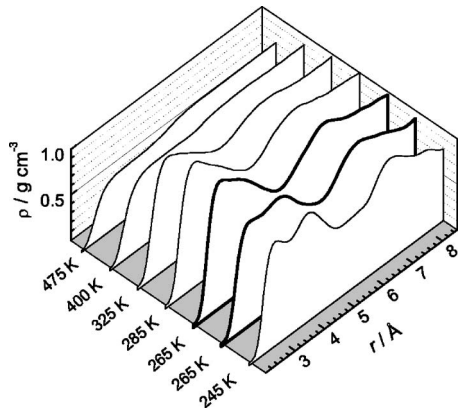


FIG. 7. Density profiles of liquid water along the liquid-vapor coexistence curve in the pore with $U_0=-0.39$ kcal/mol. Profiles of the two phases of liquid water, coexisting at $T=265$ K, are shown by thick lines. $r$ is the distance to the pore wall.

a bulk (see lower panel in Fig. 5), its temperature remains practically the same, whereas it is by about 15° higher for ST2RF water. The glass transition temperature of ST2 water in the pore with $U_0=-3.08$ kcal/mol is close to the bulk value, whereas it is higher by about 20° for ST2RF water.

### B. Structural properties of water in pores

Density profiles of liquid water in the hydrophobic pore at various temperatures along the liquid-vapor coexistence curve are shown in Fig. 7. Profiles of two liquid phases coexisting at 265 K differ noticeably. In the higher-temperature (higher-density) water phase, there is a maximum of the density profile at about 2.9 Å and a shoulder at about 3.6 Å from the pore wall. In the lower-temperature (lower-density) phase, the maximum at 2.9 Å drops, whereas the second maximum at about 3.9 Å appears. Such redistribution of water molecules within the first water layer shows, that some water molecules move away from the surface due to the liquid-liquid phase transition upon cooling. Evolution of the density profiles of the higher-temperature water phase upon heating is typical for liquids near the weakly attractive surfaces. Depletion of the water density near the hydrophobic surface (see profiles at 400 and 475 K in Fig. 7) is governed by the correlation length and intensifies with the increasing temperature.[40–42]

In the moderately hydrophilic pore, density profiles of water do not change qualitatively, when water undergoes a liquid-liquid phase transition (Fig. 8). In a wide temperature range, two pronounced density oscillations indicate presence of two ordered water layers near the pore wall. In a strongly hydrophilic pore, localization of water molecules in these two layers enhances, but basic features of the density profiles remain unchanged (Fig. 9). We have defined water molecules, which belong to the surface layer, using the average location of the first minimum of the density profiles at various temperatures. If water oxygen is located closer than 5 Å to the wall in the hydrophobic pore or closer than 4.5 Å in hydrophilic pores, the molecule was assigned to the surface layer. All other molecules are considered as located in the pore interior, that is near the pore center.

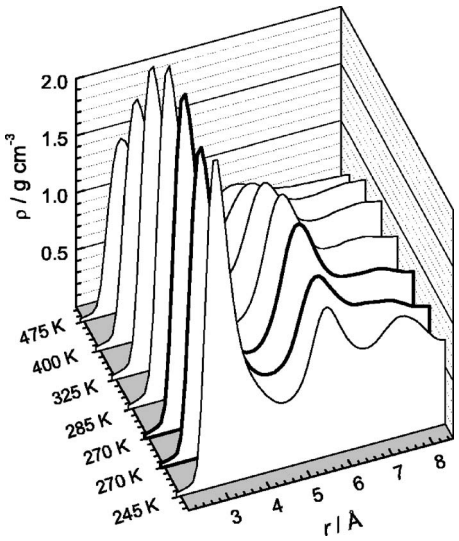


FIG. 8. Density profiles of liquid water along the liquid-vapor coexistence curve in the pore with $U_0=-1.93$ kcal/mol. Profiles of the two phases of liquid water, coexisting at $T=270$ K, are shown by thick lines. $r$ is the distance to the pore wall.

We have calculated temperature dependence of the water density in the pore center and in the surface layer along the liquid-vapor coexistence curve (Fig. 10). Above the temperature of the liquid-liquid transition, the density of liquid water in the pore center (Fig. 10, upper panel) decreases with increasing water-wall interaction in accordance with theoretical expectations for liquid-vapor transition.[43] At higher temperatures, depletion of density near hydrophobic walls extends further from the wall and causes a decrease of its average value in the pore center. The water density in the surface layers was calculated, assuming, that volume within 1.25 Å from the walls is not accessible for water molecules.

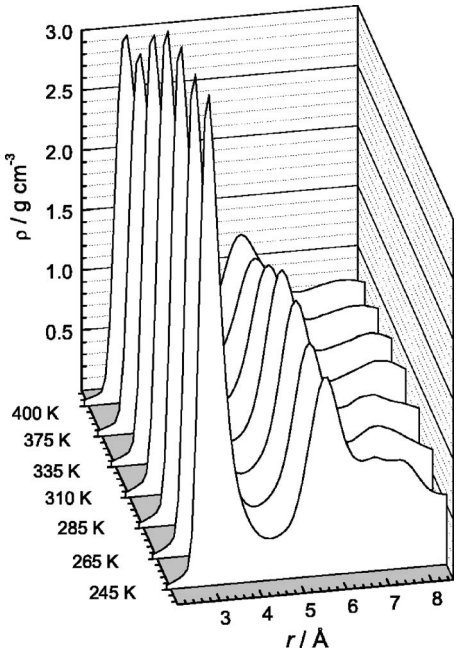


FIG. 9. Density profiles of liquid water along the liquid-vapor coexistence curve in the pore with $U_0=-3.08$ kcal/mol. $r$ is the distance to the pore wall.

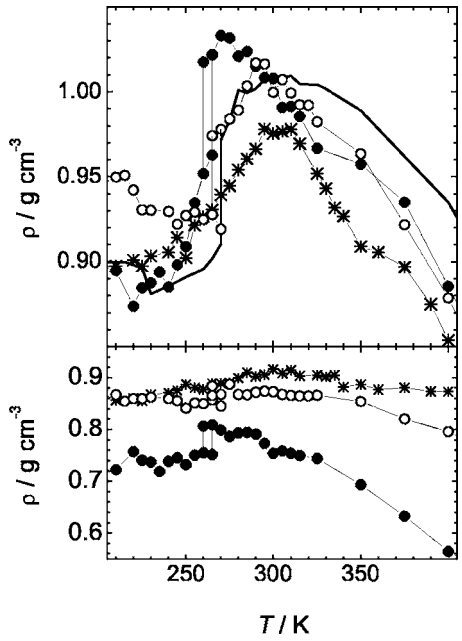


FIG. 10. Density of liquid water along the liquid-vapor coexistence curve: bulk water (thick line), water in the pore with $U_0=-0.39$ kcal/mol (closed circles), $U_0=-1.93$ kcal/mol (open circles), and $U_0=-3.08$ kcal/mol (asterisks). Upper panel: water in the pore center. Lower panel: water in the surface layer.

Such an estimated density in the surface layer can be used for the comparison of the water density in different pores, but not for the comparison with the density of bulk water. Near hydrophilic surfaces, the water density does not change noticeably within a wide temperature interval, including the temperature of the liquid-liquid transition (asterisks and open circles in the lower panel of Fig. 10). In hydrophobic pore, there is a pronounced drop of water density in a surface layer due to the liquid-liquid transition (closed circles in the lower panel of Fig. 10).

Pair correlation functions $g_{O-O}(r)$ between water oxygens in the surface layer in all three studied pores at various temperatures are shown in Fig. 11 together with $g_{O-O}(r)$ for bulk water. A wide second maximum of $g_{O-O}(r)$ of bulk water at high temperatures contains contribution from the "tetrahedral correlation" at 4.5 Å, indicating tetrahedral arrangement of three water molecules, and contribution from the "linear correlation" at 5.4 Å, which reflects a linear arrangement of three water molecules. Note, that the linear correlation becomes dominant in the supercritical region of bulk water.[44] The linear correlation between water molecules near the hydrophilic surfaces dominates at high and ambient temperatures and remains noticeable at low temperatures (Fig. 11). Localization of water molecules near the hydrophobic surface is much weaker, and $g_{O-O}(r)$ in the surface layer is closer to the bulk liquid water with a dominating tetrahedral correlation within the two coordination shells.

Distributions of the tetrahedricity parameter $\theta$ in a liquid water phase at various temperatures along the liquid-vapor coexistence curve of bulk ST2 water and ST2 water in a hydrophobic pore are shown at two left panels of Fig. 12. The left and right peaks of these distributions correspond to the tetrahedral and essentially isotropic distributions of the

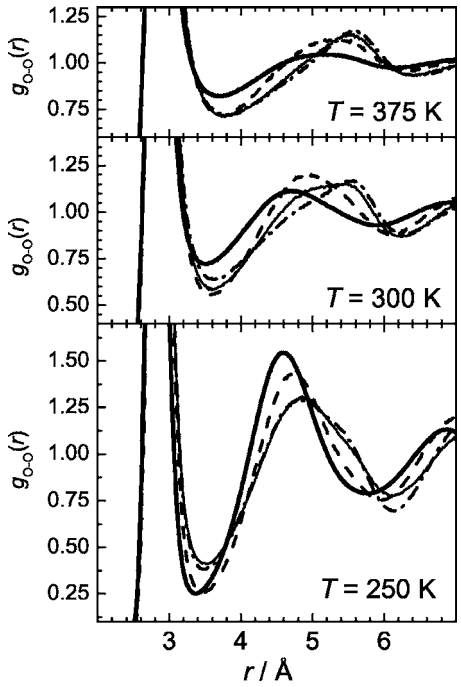


FIG. 11. Pair correlation functions $g_{O-O}$ of water in the first surface layer in the pore with $U_0=-0.39$ kcal/mol (dashed lines), $U_0=-1.93$ kcal/mol (thin solid lines), and $U_0=-3.08$ kcal/mol (dot-dashed lines). Functions $g_{O-O}$ of bulk water is shown by thick solid lines.

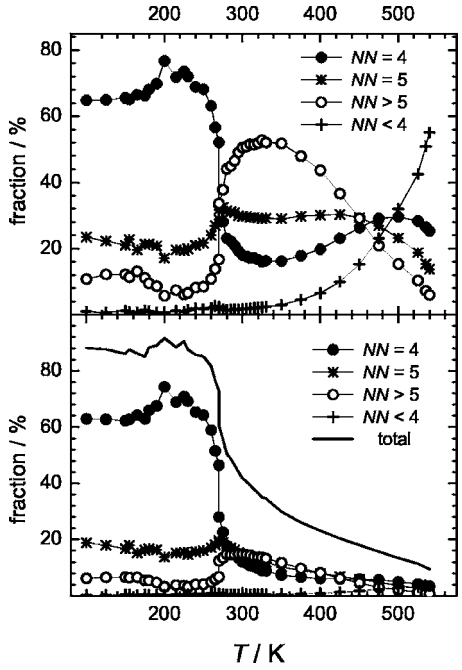


FIG. 13. Fraction of the molecules with *NN* nearest neighbors (upper panel) and the fraction of molecules with *NN* nearest neighbors and a tetrahedral arrangement of the four nearest neighbors (lower panel) in liquid water as a function of temperature along the liquid-vapor coexistence curve of bulk ST2 water.

four nearest neighbors, respectively. The pronounced two-peak structure of these distributions in a wide temperature range allows the establishing of a criterion ($\theta<0.06$) for tetrahedrally ordered water molecules. Note that probability distributions of $\theta$ is qualitatively similar for bulk water and for water in the center of hydrophobic (Fig. 12) and hydrophilic (not shown) pores. Possibility of the tetrahedral arrangement of the four nearest neighbors unavoidably diminishes in the surface layer due to the missing neighbor effect. Accordingly, the right peak in the probability distribution of the tetrahedricity parameter $\theta$ becomes dominant near pore walls (right panels in Fig. 12). Near the hydrophobic surface, the tetrahedral arrangement remains important, whereas it may be noticed at the lowest studied temperatures only near the hydrophilic surface. Note, that the distribution of the tetrahedricity parameter $\theta$ of the surface water becomes narrower upon the strengthening of the water-wall interaction. This trend evidences orientational ordering of water molecules near hydrophilic surfaces, which accompanies growing localization of water molecules near the surface.

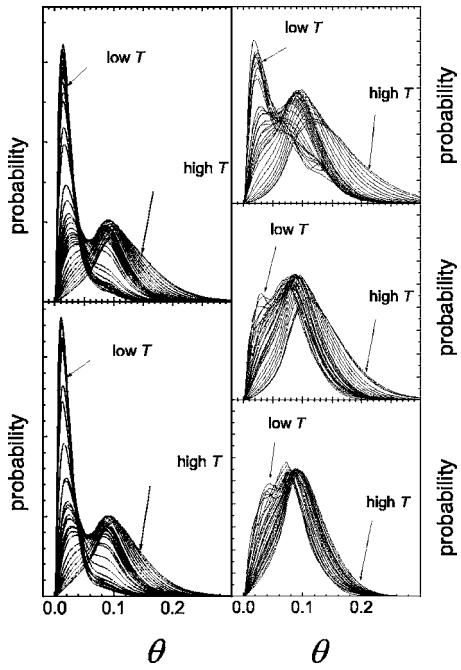


FIG. 12. Probability distributions of the tetrahedricity parameter $\theta$ of water molecules. Left panels: In bulk liquid (upper panel) and in the center of the pore with $U_0=-0.39$ kcal/mol (lower panel). Right panels: In the surface layer in the pore with $U_0=-0.39$ kcal/mol (upper panel), $U_0=-1.93$ kcal/mol (middle panel), and $U_0=-3.08$ kcal/mol (lower panel).

Liquid-liquid phase transition of ST2 water upon cooling is accompanied by the percolation transition of tetrahedrally ordered four-coordinated water molecules.[11] Therefore, it is worth analyzing the fraction of water molecules with different coordination numbers *NN* and with a different degree of tetrahedral ordering. In bulk ST2 water, the fraction of water molecules with $NN<4$ is negligible at low temperatures and grows sharply at $T>350$ K (pluses in the upper panel of Fig. 13). The fraction of molecules with $NN=4$ attains the minimum at about 340 K and shows a drastic steplike increase at $T=270$ K due to the liquid-liquid phase transition (closed circles in the upper panel of Fig. 13). This steplike increase of the fraction of the four-coordinated water molecules is accompanied by a symmetrical steplike decrease of the fraction of molecules with $NN>5$ (open circles in the upper panel of Fig. 13). Interestingly, fractions of these two species (molecules with $NN=4$ and molecules with $NN>5$) vary in antiphase in a wide temperature range, excluding the highest

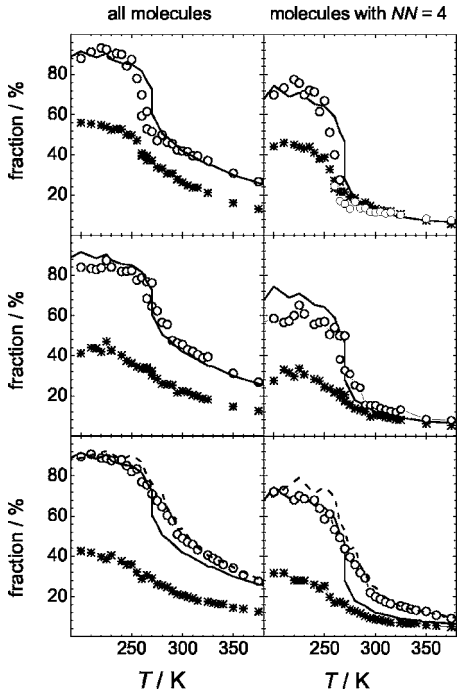


FIG. 14. Fraction of the molecules with a tetrahedral arrangement of the four nearest neighbors in liquid water as a function of temperature along the liquid-vapor coexistence. Results for ST2 water in pores with $U_0=-0.39$ kcal/mol, $U_0=-1.93$ kcal/mol, and $U_0=-3.08$ kcal/mol are shown in the upper, middle and lower panels, respectively. Results for bulk ST2 water and bulk ST2RF water are shown by solid and dashed lines, respectively. Results for water in the pore center and in the surface layer are shown by open circles and asterisks, respectively.

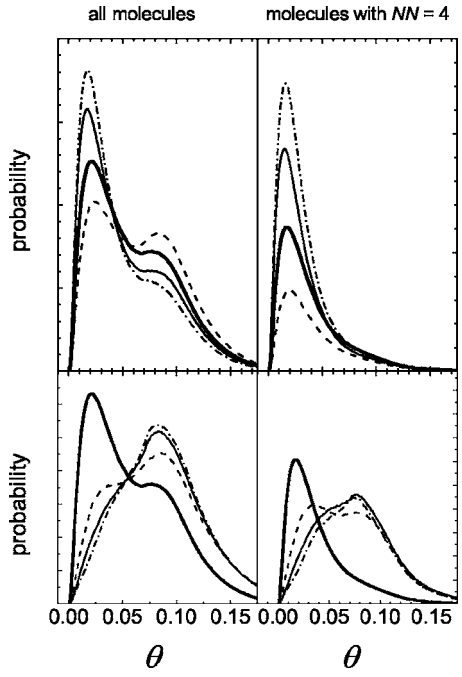


FIG. 15. Probability distributions of the tetrahedricity parameter $\theta$ for water molecules in the pore with $U_0=-0.39$ kcal/mol (dashed lines), $U_0=-1.93$ kcal/mol (thin solid lines), and $U_0=-3.08$ kcal/mol (dot-dashed lines) and in bulk liquid water (thick solid lines) at $T=275$ K. Upper panels: Water in the pore center. Lower panels: Water in the surface layer.

temperatures, where this behavior is distorted by the growing fraction of molecules with $NN<4$. The observed correlation clearly indicates a temperature-induced interconversion between these two species. Surprisingly, water molecules with $NN=5$ seem to be apart from this interconversion. Their fraction varies only slightly in a wide temperature range and does not show a step-wise change at the liquid-liquid phase transition at $T=270$ K (asterisks in the upper panel of Fig. 13).

The fraction of tetrahedrally ordered water molecules in bulk ST2 water increases with the decreasing temperature, changes in a steplike fashion at the liquid-liquid phase transition and achieves saturation (about 90%) at low temperatures (thick line in the lower panel of Fig. 13). Below the temperature of the liquid-liquid transition, more then 95% of the four-coordinated molecules have the tetrahedral arrangement of the four neighbors. This percentage is about 80% for molecules with $NN=5$, about 50% for molecules with $NN>5$ and about 40% for molecules with $NN<3$. Therefore, the four-coordinated terahedrally ordered molecule is a dominating water species in the low-temperature bulk liquid phase of water.

The temperature dependences of the fraction of water molecules, having a tetrahedral arrangement of the four nearest neighbors, are shown in the left panels of Fig. 14. In the centers of the studied pores (open circles in Fig. 14), these dependences are close to the one for bulk ST2 water (solid lines in Fig. 14). In the strongly hydrophilic pore, this dependence becomes close to the one for bulk ST2RF water. Note smaller fraction of tetrahedrally ordered molecules at low temperatures for water in the moderately hydrophilic pore. This correlates with the largest density of the low-temperature water phase in this pore (Fig. 10). Fraction of the tetrahedrally ordered molecules is essentially smaller near the surface (asterisks in the left panels of Fig. 14). Upon cooling, a steplike increase of this fraction at the liquid-liquid phase transition may be noticed in the hydrophobic pore, whereas it increases in a continuous way in hydrophilic pores.

The fraction of the four-coordinated tetrahedrally ordered water molecules in the centers of the hydrophobic and moderately hydrophilic pores shows a steplike increase at the liquid-liquid transition (open circles in the upper and middle panels in Fig. 14). In the strongly hydrophilic pore, where the liquid-liquid phase transition does not occur at zero pressure, this fraction grows in a continuous way upon cooling (open circles in the lower panel in Fig. 14). A qualitatively similar temperature dependence is observed for bulk ST2RF water (dashed line in the lower panel in Fig. 14). In the surface layer, a steplike increase of the fraction of the four-coordinated tetrahedrally ordered water molecules may be noticed for the hydrophobic pore only. Note, that in all of the pores the four-coordinated water molecule with the tetrahedral arrangement of the nearest neighbors is a dominant species of the low-temperature liquid phase, as in the bulk water.

The probability distributions of the tetrahedricity parameter $\theta$ of water in three studied pores and in the bulk are compared in Fig. 15 at $T=275$ K, that is just above the temperature of the liquid-liquid transition. Tetrahedral ordering of all water molecules, and the tetrahedral ordering of the

four-coordinated molecules in particular, is lower in the center of the hydrophobic pore in comparison with the bulk water, whereas it is higher in the centers of the hydrophilic pores (upper panels in Fig. 15). In the surface layer, tetrahedral ordering is always lower, than in the bulk (lower panels in Fig. 15). Note, that fraction of water molecules in the surface layer with the tetrahedral arrangement of the four nearest neighbors is noticeable in the hydrophobic pore only. Tetrahedral ordering in liquid water is strongly sensitive to its density.[10] The decreasing of the liquid water density in the centers of the hydrophilic pores (Fig. 10) may explain the improvement of the tetrahedral ordering of water in their centers.

## IV. DISCUSSION

We have found, that the liquid-liquid phase transition of model water, seen in the bulk system, occurs also when water is confined in rather narrow pores. This finding strongly indicates, that the liquid-liquid transition of water should be taken into account, when analyzing various properties of confined water, including its dynamic transition in the supercooled region. Obviously, the two liquid phases of a different density and structure should also differ in dynamical properties and a qualitative change of dynamics should be expected due to the liquid-liquid phase transition. Moreover, such a qualitative change may be expected also upon crossing the Widom line not very far from the critical point. Therefore, our results are evidence of the attribution of the dynamic transition of supercooled confined water to the liquid-liquid transition.[8,18,19,29]

The temperature $T_t$ of the liquid-liquid-vapor triple point or the temperature of the heat capacity maximum of confined model water shifts by just $10°-15°$ from the bulk value, when the pore walls change from strongly hydrophobic to strongly hydrophilic. This agrees with experimentally observed robustness of the temperature of the dynamic and/or liquid-liquid transition of water with respect to various confinements, including the surface of biomolecules. The transition line of the first liquid-liquid transition of water is characterized by the large values of $dP/dT$ (about 4 kbar per 100°, as was estimated from experiment[45] and simulations[6,7]). This slope is much smaller for the liquid-vapor transition and pressure of the liquid-vapor coexistence changes in a rather narrow interval due to confinement. The lines of both phase transitions in the pressure-temperature plane shift in pores, and for the first approximation this shift may be considered as a parallel displacement along the pressure axis. The crossing point of these two lines, with very different slopes, changes only slightly when they undergo parallel displacements within some reasonable range of pressure. Therefore, very different slopes of the lines of the liquid-vapor and liquid-liquid transitions in the pressure-temperature plane seem to be responsible for the robustness of the liquid-liquid transition of water with respect to various confinements.

The shift of $T_t$ to lower temperatures due to confinement in hydrophobic pores indicates, that the hydrophobic surface promotes a less ordered higher-density phase of liquid water. Two main factors may be responsible for such behavior. First, this trend reflects the disordering effect of the hydrophobic surface on liquid water: The number of hydrogen bonds decreases (as near any surface), the potential energy worsens, and the dynamics of water are enhanced.[46] Second, the density of a liquid water in the center of the hydrophobic pore is always higher the density of bulk liquid water at the same temperature[42] (see also Fig. 10). A larger density suppresses the fraction of the four-coordinated molecules and decreases the tetrahedral ordering[10] (see also Fig. 15), which are dominant in the low-temperature phase of liquid water, thus requiring the lower temperature for the phase transition. In the hydrophilic pore, water density in its center is always lower then the density of bulk liquid, that promotes four-coordinated molecules and shifts the liquid-liquid transition to higher temperature. Besides, the strong orientational ordering of water molecules near a hydrophilic surface may additionally promote a more ordered lower-density water phase, providing the positive shift of $T_t$.

The shift of $T_t$ to higher temperatures with increasing pore hydrophilicity was obtained for water in pores with model structureless walls. Depletion of water near smooth and structured hydrophobic surfaces are rather similar. Hydrogen bonds between water molecules and the hydrophilic surface, absent in our model system, cause additional orientational orderings of surface water, that may lead to the further increase of $T_t$. Therefore, we do not expect, that the general trends in the behavior of $T_t$ may differ qualitatively for water near smooth and structured surfaces. The observed trends agree with the higher temperature of the liquid-liquid transition of water in the hydrophilic Vycor glass (~240) (Refs. 16 and 17) and in the silica pores (~225 K) (Refs. 18, 19, and 21) in comparison with the less hydrophilic carbon nanotubes (~218 K).[24] The temperature shift of the liquid-liquid transition in pores correlates with an even larger shift of the temperature of the liquid density maximum (see Fig. 10). This correlation agrees with the observed shift of both the liquid density maximum and the liquid-liquid transition to lower temperatures in a very narrow hydrophobic pore.[36]

The shift of the liquid-liquid critical point of water from a negative pressure in the bulk to positive pressure in the strongly hydrophilic pore with $U_0=-3.08$ kcal/mol may be also attributed to the lowering of the water density in the pore center in comparison with a bulk value and to the strong enhancement of the orientational ordering of water molecules near smooth hydrophilic surfaces.[38] Enhancement of the orientational ordering of water molecules due to the application of the long-range corrections for the Coulombic interaction causes qualitatively similar shift of the liquid-liquid transition of bulk water.[6] Besides, the same shift was observed in the simple van der Waals model of hydrogen-bonded liquid due to the strengthening of the hydrogen bonds.[13] The critical point of the phase transition with negative $dP/dT$ may also be shifted from a negative to positive pressure due to the decrease of its critical temperature in confinement. The pore size becomes effectively narrower, when strongly adsorbed water layer(s) are not affected by the liquid-vapor phase transition.[38] We cannot exclude, that simi-

lar effect causes effective narrowing of the strongly hydrophilic pore also for the liquid-liquid transition.

We have found that the liquid-liquid transition affects the density and structure of water near the surface weaker than in the bulk. This general trend should be attributed to the effect of the missing neighbor, that affects any phase transition near the boundary and diminishes the difference between the coexisting phases. Noticeable changes in the water structure due to the liquid-liquid transition are observed near a hydrophobic surface. In particular, a decrease of water density promotes tetrahedral ordering near the surface and water molecules shift further from the surface within the surface layer. These changes are much smaller near the moderately hydrophilic wall and disappears near the strongly hydrophilic wall. Therefore, we expect that the liquid-liquid transition of water near heterogeneous biological surfaces to affect the stronger water near their hydrophobic parts. Note, that this transition should affect water properties near hydrophilic parts at higher temperatures.

The four-coordinated water molecules with tetrahedrally arranged nearest neighbors are found to be the dominating species in the low-temperature water phase of bulk (Fig. 13) and confined (Fig. 14) water. When approaching the wall, the fraction of the four-coordinated molecules decreases (due to the missing neighbor effect), whereas the fraction of the three-coordinated molecules with the perfect arrangement of the four nearest neighbors essentially increases. A specific behavior of five-coordinated water molecules is observed in the bulk water (Fig. 13), as well as for the water in the pore centers (not shown). The fraction of these species remains very stable (20%–30%) in a wide temperature interval, which includes the liquid-liquid transition. In contrast, the fractions of the four-coordinated molecules and molecules with $NN>5$ change drastically in the same temperature interval. A temperature change causes interconversion between molecules with $NN>5$ and molecules $NN=4$, but this process does not affect noticeably molecules with $NN=5$. Interestingly, similar redistribution between the fractions of these three water species occurs also with the increasing water density (up to 1.1 $g/cm^{-3}$ at $T=200$ K).[10]

Based on the obtained results, we want to propose experiments, which may help to clarify at what pressure (positive or negative) the liquid-liquid critical point is located in real water. Experiments with water in incompletely filled pores[16,17] is clear evidence of a first-order phase transition at zero pressure, and indicates the critical point at negative pressures. In experiments with water in cylindrical mesopores,[18,19] clear evidences of the liquid-liquid transition at zero pressure were not found and dynamic transition of water was attributed to the crossing of the Widom line, emanating from the liquid-liquid critical point at a positive pressure. Our results indicate, that the location of the liquid-liquid phase transition and its critical point in pores may be affected by varying hydrophilicity/hydrophobicity of the pore surface. In particular, the liquid-liquid critical point may be placed exactly at the liquid-vapor coexistence curve (i.e., at zero pressure) by tuning the strength of the water-wall interaction (see Fig. 1). The experimental realization of such a scenario should make the hypothesized liquid-liquid critical point of water more accessible to various experimental methods.

## ACKNOWLEDGMENT

We thank the Deutsche Forschungsgemeinschaft for financial support.

[1] P. G. Debenedetti, J. Phys.: Condens. Matter **15**, R1669 (2003).
[2] P. H. Poole, F. Sciortino, U. Essmann, and H. E. Stanley, Nature **360**, 324 (1992).
[3] O. Mishima, L. D. Calvert, and E. Whalley, Nature **314**, 76 (1985).
[4] T. Loerting, W. Schustereder, K. Winkel, C. G. Salzmann, I. Kohl, and E. Mayer, Phys. Rev. Lett. **96**, 025702 (2006).
[5] I. Brovchenko, A. Geiger, and A. Oleinikova, J. Chem. Phys. **118**, 9473 (2003).
[6] I. Brovchenko, A. Geiger, and A. Oleinikova, J. Chem. Phys. **123**, 044515 (2005).
[7] P. H. Poole, I. Saika-Voivod, and F. Sciortino, J. Phys.: Condens. Matter **17**, L431 (2005).
[8] L. Xu, P. Kumar, S. V. Buldyrev, S.-H. Chen, P. H. Poole, F. Sciortino, and H. E. Stanley, Proc. Natl. Acad. Sci. U.S.A. **102**, 16558 (2005).
[9] F. H. Stillinger and A. Rahman, J. Chem. Phys. **60**, 1545 (1974).
[10] I. Brovchenko and A. Oleinikova, J. Chem. Phys. **124**, 164505 (2006).
[11] A. Oleinikova and I. Brovchenko, J. Phys.: Condens. Matter **18**, S2247 (2006).
[12] I. Brovchenko and A. Oleinikova, in *Proceedings of the 11th International Conference on the Physics and Chemistry of Ice* (Royal Society of Chemistry, Cambridge, England, 2007), p. 117.
[13] P. H. Poole, F. Sciortino, T. Grande, H. E. Stanley, and C. A. Angell, Phys. Rev. Lett. **73**, 1632 (1994).
[14] T. Takamuku, M. Yamagami, H. Wakita, Y. Masuda, and T. Yamaguchi, J. Phys. Chem. B **101**, 5730 (1997).
[15] A. Schreiber, I. Ketelsen, and G. H. Findenegg, Phys. Chem. Chem. Phys. **3**, 1185 (2001).
[16] J.-M. Zanotti, M.-C. Bellissent-Funel, and S.-H. Chen, Europhys. Lett. **71**, 91 (2005).
[17] J.-M. Zanotti, M. C. Bellissent-Funel, S.-H. Chen, and A. I. Kolesnikov, J. Phys.: Condens. Matter **18**, S2299 (2006).
[18] A. Faraone, L. Liu, C.-Y. Mou, C.-W. Yen, and S.-H. Chen, J. Chem. Phys. **121**, 10843 (2004).
[19] L. Liu, S.-H. Chen, A. Faraone, C.-W. Yen, and C.-Y. Mou, Phys. Rev. Lett. **95**, 117802 (2005).
[20] L. Liu, S.-H. Chen, A. Faraone, C. Y. Mou, A. I. Kolesnikov, E. Mamontov, and J. Leno, J. Phys.: Condens. Matter **18**, S2261 (2006).
[21] F. Mallamace, M. Broccio, C. Corsaro, A. Faraone, U. Wanderlingt, L. Liu, C.-Y. Mou, and S.-H. Chen, J. Chem. Phys. **124**, 161102 (2006).
[22] F. Mallamace, M. Broccio, C. Corsaro, A. Faraone, L. Liu, C.-Y. Mou, and S.-H. Chen, J. Phys.: Condens. Matter **18**, S2285 (2006).
[23] D. W. Hwang, C.-C. Chu, A. K. Sinha, and L.-P. Hwang, J. Chem. Phys. **126**, 044702 (2007).
[24] E. Mamontov, C. J. Burnham, S.-H. Chen, A. P. Moravsky, C.-K. Loong, N. R. de Souza, and A. I. Kolesnikov, J. Chem. Phys. **124**, 194703 (2006).
[25] S.-H. Chen, L. Liu, X. Chu, Y. Zhang, E. Fratini, P. Baglioni, A. Faraone, and E. Mamontov, J. Chem. Phys. **125**, 171103 (2006).
[26] S.-H. Chen, L. Liu, E. Fratini, P. Baglioni, A. Faraone, and E. Mamontov, Proc. Natl. Acad. Sci. U.S.A. **103**, 9012 (2006).
[27] P. W. Fenimore, H. Frauenfelder, B. H. McMahon, and F. G. Parak, Proc. Natl. Acad. Sci. U.S.A. **99**, 16047 (2002).
[28] G. Caliskan, R. M. Briber, D. Thirumalai, V. Garcia-Sakai, S. A. Woodson, and A. P. Sokolov, J. Am. Chem. Soc. **128**, 32 (2006).
[29] P. Kumar, Z. Yan, M. G. Mazza, S. V. Buldyrev, S.-H. Chen, S. Sastry, and H. E. Stanley, Phys. Rev. Lett. **97**, 177802 (2006).
[30] K. Ito, C. T. Moynihan, and C. A. Angell, Nature **398**, 492 (1999).
[31] J. Swenson, Phys. Rev. Lett. **97**, 189801 (2006).
[32] S. Cerveny, J. Colmenero, and A. Alegria, Phys. Rev. Lett. **97**, 189802 (2006).
[33] S.-H. Chen, L. Liu, and A. Faraone, Phys. Rev. Lett. **97**, 189803 (2006).
[34] T. M. Truskett, P. G. Debenedetti, and S. Torquato, J. Chem. Phys. **114**, 2401 (2001).
[35] M. Meyer and H. E. Stanley, J. Phys. Chem. B **103**, 9728 (1999).

[36] P. Kumar, S. V. Buldyrev, F. W. Starr, N. Giovambattista, and H. E. Stanley, Phys. Rev. E **72**, 051503 (2005).
[37] A. Z. Panagiotopoulos, Mol. Phys. **61**, 813 (1987).
[38] I. Brovchenko, A. Geiger, and A. Oleinikova, J. Chem. Phys. **120**, 1958 (2004).
[39] Y. I. Naberukhin, V. P. Voloshin, and N. N. Medvedev, Mol. Phys. **73**, 917 (1991).
[40] I. Brovchenko, A. Geiger, and A. Oleinikova, J. Phys.: Condens. Matter **16**, S5345 (2004).
[41] I. Brovchenko, A. Geiger, and A. Oleinikova, Eur. Phys. J. B **44**, 345 (2005).
[42] I. Brovchenko and A. Oleinikova, *Handbook of Theoretical and Computational Nanotechnology* (American Scientific Publishers, Stevenson Ranch, CA, 2006), Vol. 9, Chap. 3, pp. 109–206.
[43] H. Nakanishi and M. E. Fisher, J. Chem. Phys. **78**, 3279 (1983).
[44] L. B. Partay, P. Jedlovszky, I. Brovchenko, and A. Oleinikova, Phys. Chem. Chem. Phys. **9**, 1341 (2007).
[45] O. Mishima, Phys. Rev. Lett. **85**, 334 (2000).
[46] I. Brovchenko, A. Geiger, A. Oleinikova, and D. Paschek, Eur. Phys. J. E **12**, 69 (2003).